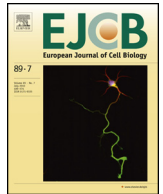




Contents lists available at ScienceDirect

European Journal of Cell Biology

journal homepage: www.elsevier.com/locate/ejcb



Research paper

Coronin 1C-free primary mouse fibroblasts exhibit robust rearrangements in the orientation of actin filaments, microtubules and intermediate filaments

Juliane Behrens^{a,1}, Roxana Solga^{a,1}, Anja Ziemann^a, Raphael H. Rastetter^{a,b,c},
Carolin Berwanger^a, Harald Herrmann^d, Angelika A. Noegel^{a,b,c}, Christoph S. Clemen^{a,*}

^a Center for Biochemistry, Institute of Biochemistry I, Medical Faculty, University of Cologne, 50931 Cologne, Germany

^b Center for Molecular Medicine Cologne (CMMC), University of Cologne, 50931 Cologne, Germany

^c Cologne Excellence Cluster on Cellular Stress Responses in Aging-Associated Diseases (CECAD), University of Cologne, 50931 Cologne, Germany

^d Institute of Neuropathology, University Hospital Erlangen, 91054 Erlangen, Germany

ARTICLE INFO

Article history:

Received 15 April 2016

Received in revised form 25 April 2016

Accepted 25 April 2016

Keywords:

CRN2

Coronin 1C

Knock-out

Migration

Actin

Vimentin

Intermediate filaments

Microtubules

Mitochondria

Primary fibroblasts

ABSTRACT

Coronin 1C is an established modulator of actin cytoskeleton dynamics. It has been shown to be involved in protrusion formation, cell migration and invasion. Here, we report the generation of primary fibroblasts from coronin 1C knock-out mice in order to investigate the impact of the loss of coronin 1C on cellular structural organisation. We demonstrate that the lack of coronin 1C not only affects the actin system, but also the microtubule and the vimentin intermediate filament networks. In particular, we show that the knock-out cells exhibit a reduced proliferation rate, impaired cell migration and protrusion formation as well as an aberrant subcellular localisation and function of mitochondria. Moreover, we demonstrate that coronin 1C specifically interacts with the non- α -helical amino-terminal domain ("head") of vimentin. Our data suggest that coronin 1C acts as a cytoskeletal integrator of actin filaments, microtubules and intermediate filaments.

© 2016 The Authors. Published by Elsevier GmbH. This is an open access article under the CC BY-NC-ND license (<http://creativecommons.org/licenses/by-nc-nd/4.0/>).

1. Introduction

Since their first description in the amoeba *Dictyostelium discoideum* (de Hostos et al., 1991), coronin proteins were studied in different model organisms. The coronin family of proteins is a group of conserved regulators of the actin cytoskeleton, which comprises seventeen coronin subfamilies including seven paralogs in mammals (Eckert et al., 2011; Morgan and Fernandez, 2008; Xavier et al., 2008). Structural characteristic of a coronin protein is the presence of a basic N-terminal signature motif (Rybakin and Clemen, 2005), followed by a WD40-repeat domain that adopts the fold of a seven-bladed β -propeller (Appleton et al., 2006; McArdle and Hofmann, 2008), a linker domain of variable length that is partially unique for a specific coronin (McArdle and Hofmann, 2008) and a

C-terminal coiled coil mediating oligomerisation (Kammerer et al., 2005; Spoerl et al., 2002).

The 474 amino acid protein coronin 1C is also known as coronin-3, hCRNN4, coronin 3 and CRN2 due to different inconsistent nomenclatures used in the literature and is referred to as CRN2 in the present study. CRN2 binds to and bundles actin filaments via different actin binding sites (Chan et al., 2012; Xavier et al., 2012). It interacts with the Arp2/3 complex and with cofilin (Rosentreter et al., 2007; Xavier et al., 2012). CRN2 is a substrate of the protein kinase CK2 (casein kinase II), which phosphorylates CRN2 at serine 463 within the coiled coil forming segment. Phosphorylated CRN2 loses its ability to inhibit actin polymerization, to bundle actin filaments and to bind to the Arp2/3 complex (Xavier et al., 2012). In glioma cells, CRN2 was found as target of the protein-tyrosine phosphatase 1B (PTP1B). Here, inhibition of PTP1B contributes to proliferation and migration probably due to maintaining tyrosine phosphorylation of CRN2 (Mondol et al., 2014). Moreover, CRN2 binds to both GDP-Rac1 and RCC2 thereby enriching GTP-Rac1 at membrane protrusions (Williamson et al., 2014), and also to GDP-

* Corresponding author at: Institute of Biochemistry I, Medical Faculty, University of Cologne, Joseph-Stelzmann-Street 52, 50931 Cologne, Germany.

E-mail address: christoph.clemen@uni-koeln.de (C.S. Clemen).

¹ Both authors contributed equally to this work.

<http://dx.doi.org/10.1016/j.ejcb.2016.04.004>

0171-9335/© 2016 The Authors. Published by Elsevier GmbH. This is an open access article under the CC BY-NC-ND license (<http://creativecommons.org/licenses/by-nc-nd/4.0/>).

Rab27a leading to inhibition of endocytosis of insulin secretory membranes for recycling (Kimura et al., 2010).

CRN2 is involved in numerous cellular processes like adhesion, protrusion and invadopodia formation, neurite outgrowth, secretion, endocytosis, matrix degradation, cytokinesis, proliferation, migration and invasion (Kimura et al., 2008; Rosentreter et al., 2007; Samarin et al., 2010; Thal et al., 2008; Williamson et al., 2014; Ziemann et al., 2013). Experimental and clinical data provide evidence that CRN2 is involved in the development of human cancer, i.e. glioblastoma (Mondol et al., 2014; Thal et al., 2008; Ziemann et al., 2013), primary effusion lymphoma (Luan et al., 2010), hepatocellular carcinoma (Wang et al., 2013; Wu et al., 2010), gastric cancer (Ren et al., 2012) and ER α /PR/HER-2 triple-negative breast cancer (Wang et al., 2014).

In the present study we determined the effects of the complete lack of CRN2 using primary skin fibroblasts derived from CRN2 knock-out mice. Besides changes in the actin cytoskeleton, the lack of CRN2 affects microtubules and the vimentin intermediate filament network. We demonstrate that CRN2 specifically interacts with the non- α -helical “head” domain of vimentin *in vitro*.

2. Materials and methods

2.1. Generation of CRN2 knock-out mice

We generated two independent CRN2 knock-out mouse strains from the ES cell clones EPD0343.2.B04 and EPD0343.2.F09, which were obtained from the NCRR-NIH supported KOMP Repository (www.komp.org) and generated by the CSD consortium for the NIH funded Knockout Mouse Project (KOMP). CRN2 gene targeting was performed according to the “knockout first allele” strategy (Testa et al., 2004). In brief, homologous recombination of the CRN2 targeting vector led to the insertion of a promoter-driven targeting construct, which comprises a lacZ reporter and a neomycin selection cassette, into intron 4 in conjunction with floxing of exon 5 (coding exon 4). Subsequently, we cross-bred animals harbouring the targeted allele (“reporter-tagged insertion”) with animals expressing Cre and Flp recombinases in order to generate reporter knock-out (“reporter-tagged deletion”), conditional knock-out (floxed coding exon 4) and knock-out (“deletion with no reporter”) mice. We used reporter-tagged insertion animals for the purpose of this study. By Southern blotting we confirmed the correct insertion of the targeting construct and, in addition, repeatedly verified its presence during maintenance of our CRN2 knock-out mouse strains. Routine genotyping of our mice with pure C57BL/6N genetic background was done by PCR (primer pair 5'-CGGTCAGTAGCCTTCTGG-3' and 5'-CCGAGGGCACTCTAAGCTGT-3') resulting in products of 286 bp for the wild-type and 240 bp for the targeted alleles. RT-PCR analyses confirmed the knock-out of CRN2 at the mRNA level. The absence of CRN2 and potential truncated protein species was further confirmed by immunoblotting using several mono- and polyclonal antibodies.

Mice were housed in isolated ventilated cages (IVC) equipped with spruce granulate embedding and a nest under specific and opportunistic pathogen-free (SOPF) conditions at a temperature of $22 \pm 2^\circ\text{C}$, an air humidity of 50–70%, a ventilation rate of 70 air exchanges per hour and a light-dark-cycle of 12/12 h with free access to water and food. Littermates were separated at weaning by sex and housed at a maximum of five animals per cage. Health monitoring was done as recommended by the Federation of European Laboratory Animal Science Associations (FELASA). Mice were handled in accordance with the German Animal Welfare Act (Tierschutzgesetz) as well as the German Regulation for the protection of animals used for experimental purposes

or other scientific purposes (Tierschutz-Versuchstierverordnung) and the investigations were approved by the responsible governmental animal care and use office (Landesamt für Natur, Umwelt und Verbraucherschutz North Rhine-Westphalia, Recklinghausen, Germany; reference number 8.87-50.10.31.09.045).

Both CRN2 knock-out mouse strains could be bred to homozygosity, were viable and did not show any obvious anomaly. In addition to our own investigation, comprehensive phenotyping at The German Mouse Clinic (GMC), Institute of Experimental Genetics, Helmholtz Zentrum München German Research Center for Environmental Health, did not detect any significant pathology. Further details on the generation of our CRN2 knock-out mice and the data obtained from the analyses of these mice will be published elsewhere.

2.2. Isolation and cultivation of primary mouse skin fibroblasts

Primary mouse fibroblasts were isolated from skin of 2–4 days old CRN2 knock-out mice of both strains (B04 and F09) as well as the respective wild-type littermates. For fibroblast isolation, mice were decapitated, kept in betaisodona solution (Mundipharma, #0448947 (PZN)) for 2 min, washed with PBS, incubated in 80% ethanol and again washed with PBS. Back and front skin was dissected, residual fat removed and the skin tissue was incubated overnight at 4°C in a 5.5 U/ml dispase II (Roche, #04942078001) solution prepared in PBS. Subsequently, the dermis was separated from the epidermis, cut into small pieces and digested in a 400 U/ml collagenase I solution in DMEM without serum for 1 h at 37°C in a shaking incubator. The resulting cell suspension was mixed with DMEM containing serum and centrifuged at 200g for 5 min. The cell pellet was re-suspended in 4 ml DMEM with serum, filtered through a $70\ \mu\text{m}$ pore cell strainer (Falcon, #352350), centrifuged at 200g for 5 min, before the cell pellet finally was re-suspended in medium and transferred to a cell culture dish. Cells were grown in Dulbecco's modified Eagle medium (DMEM) supplemented with 10% FCS, 100 U/ml penicillin, 100 $\mu\text{g}/\text{ml}$ streptomycin, non-essential amino acids (100 μM each), 2 mM L-Glutamine and 1 mM sodium pyruvate at 37°C and 5% CO_2 . Cells were split daily after reaching confluence and passages up to 6 were used for the experiments.

2.3. Analysis of cell proliferation and migration

To determine proliferation rates, 7×10^4 fibroblasts were seeded in duplicate into 60 mm diameter culture dishes. After 24 and 48 h they were trypsinised and counted. Cell migration was analysed employing an *in vitro* wound healing assay. For each cell line 50,000 cells in $70\ \mu\text{l}$ medium containing 0.5% newborn calf serum (NBCS) were seeded in both wells of the silicone inserts (growth area $0.22\ \text{cm}^2$ per well; Ibidi, #80209) placed inside μ -slide 8-well chambers (Ibidi, #80826). After cell attachment, the insert was removed creating a defined cell free gap of $500\ \mu\text{m}$. Cell migration into the gap was started by adding $200\ \mu\text{l}$ medium containing 10% NBCS per well and observed by live cell imaging using time lapse microscopy under controlled culture conditions with a humidified atmosphere at 37°C and 5% CO_2 . Images were captured every 15 min for 24 h. For assay analysis, single cells were tracked using the Manual Tracking plugin (Fabrice Cordelières, Institut Curie, Orsay, France) of the ImageJ software (NIH). After tracking, the cell paths were analysed using the Chemotaxis and Migration tool (Ibidi) to compute the accumulated distance (mean distance of all cell paths). Velocity of the cells was calculated by dividing accumulated distance (in μm) by migration time (in sec); directionality by dividing the euclidean by the accumulated distance.

Download English Version:

<https://daneshyari.com/en/article/8469739>

Download Persian Version:

<https://daneshyari.com/article/8469739>

[Daneshyari.com](https://daneshyari.com)